Materials Today: Proceedings 57 (2022) 1315–1321

Contents lists available at ScienceDirect

Materials Today: Proceedings

journal homepage: www.elsevier.com/locate/matpr

Photocatalytic degradation of methylene blue using ZnO supported on wood waste-derived activated carbon (ZnO/AC)

J.Y. Loke [a], R.S. Mohd Zaki [b], H.D. Setiabudi [b,c,*]

[a] Department of Chemical Engineering, College of Engineering, Universiti Malaysia Pahang, Lebuhraya Tun Razak, 26300 Gambang, Pahang, Malaysia
[b] Faculty of Chemical and Process Engineering Technology, Universiti Malaysia Pahang, Lebuhraya Tun Razak, 26300 Gambang, Pahang, Malaysia
[c] Centre of Excellence for Advanced Research in Fluid Flow, Universiti Malaysia Pahang, Lebuhraya Tun Razak, 26300 Gambang, Pahang, Malaysia

ARTICLE INFO

Article history:
Available online 19 January 2022

Keywords:
ZnO/AC
Photocatalyst
Methylene blue
Activated carbon
Photocatalytic

ABSTRACT

This study reports the preparation of ZnO supported on wood waste-derived activated carbon (ZnO/AC) and its activity towards photocatalytic degradation of methylene blue (MB). The removal of MB is imperative owing to its toxic impacts on the receiving water bodies. Thus, finding treatment techniques with criteria of efficient, cost-effective, and environmentally benign is highly needed. ZnO/AC has been synthesized by the incipient wetness impregnation method and was characterized using XRD, FTIR, PL, and UV–Vis-NIR. Characterization analysis revealed the successful impregnation of ZnO onto the AC. The best photocatalytic degradation of MB using ZnO/AC was achieved at 180 min, adsorbent dosage of 3 g/L, and pH 8. Complete MB degradation was attained at lower initial MB concentrations (10 – 50 mg/L) and slightly decreased at higher initial MB concentration (100 mg/L). The experimental data fitted well with the pseudo-first-order Langmuir-Hinshelwood kinetic model with a correlation coefficient (R^2) greater than 0.995. The results revealed that the synthesized ZnO/AC exhibited remarkable photocatalytic activity towards the degradation of MB.

Selection and peer-review under responsibility of the scientific committee of the International Symposium of Reaction Engineering, Catalysis & Sustainable Energy.

1. Introduction

In recent years, wastewater treatment has gained significant attention due to the high toxicity of the containing pollutants, which can seriously damage the environment. Dyes were used extensively at various commercial levels, mainly in the textile, cosmetics, leather, and paper sectors [1]. It is anticipated that the annual production of dye is more than 700,000 tons, and approximately 12% of the dye is released as untreated effluents [2]. Among others, methylene blue (MB) is extensively used in industries, and the exposure of MB can result in vomiting, eye infection, diarrhea, nausea, cyanosis, jaundice, quadriplegia, and tissue necrosis [3]. Hence, it is imperative to remove MB from the wastewater.

Conventional treatment such as coagulation [4] and adsorption [5] are the traditional methods used to remove the dyes. However, these processes will lead to secondary hazardous pollution since this method converts liquid phase pollutants into solid-phase pollutants [6]. Consequently, researchers have developed several techniques to treat wastewater with criteria of efficient, cost-effective, and environmentally benign. Among others, photocatalytic degradation of dyes is one of the most widely used methods [7]. Various metal oxide-based semiconductors have been employed as photocatalyst for wastewater treatment, including Fe_2O_3 [8], CuO [9], TiO_2 [10], RuO_2 [11], NiO [12], ZnO [13], CeO_2 [14], and Cr_2O_3 [15,16]. In previous studies, TiO_2 stands out as the most effective photocatalyst and has been extensively used in water and wastewater treatment studies as it is thermally stable, cost-effective, chemically and biologically inert, non-toxic, and capable of promoting the oxidation of organic compounds [17,18]. However, recent studies have shown that the performances of ZnO as photocatalyst are much more efficient compared to TiO_2 as the absorption of the solar spectrum of ZnO is in a larger fraction than TiO_2 [19]. Besides, ZnO has higher electron mobility and lifetime as well as relatively lower production costs than TiO_2, causing ZnO to be a considerably suitable semiconductor for the photocatalytic process [20]. Apart from that, ZnO has attracted more attention due to its abundant availability, biocompatible, high stability, direct energy bandgap (3.37 eV), and large excitation binding energy (60 meV) [16].

* Corresponding author.
E-mail address: herma@ump.edu.my (H.D. Setiabudi).

https://doi.org/10.1016/j.matpr.2021.12.535

Selection and peer-review under responsibility of the scientific committee of the International Symposium of Reaction Engineering, Catalysis & Sustainable Energy.

For the selection of supporting materials, activated carbon has been widely utilized as a support for heterogeneous catalysis as well as in various applications. This is due to its vast surface area, high degree of surface reactivity, and microporous structure. Hence, activated carbon has a prominent effect on the adsorption of contaminants from an aqueous environment [21]. However, the high expense of coal-based activated carbon has prompted a study for alternate activated carbon sources, including agricultural wastes such as coconut shells [22], stalks [23], jackfruit peel [24], and wood wastes [25]. Wood wastes have been listed as one of the abundant wastes in Malaysia, which are estimated to generate around 2.27 million tonnes of wastes per year. Interestingly, the carbon content of wood wastes is greater than 47%, which makes these materials suitable for the preparation of activated carbon [25].

Recently, our research group [25] has successfully prepared wood waste-derived activated carbon (AC) that possessed unique properties that allowed it to be used as a low-cost activated carbon for wastewater treatment. The prepared AC demonstrated high efficiency in lead (Pb(II)) adsorption with an ideal Pb(II) update of 149.25 mg/g. The effectiveness of AC was shown by its great performance in the reusability investigation of five cycles. Impressed with the superb performance of AC in the adsorption process, the photocatalytic degradation of methylene blue utilizing ZnO supported on wood-waste derived activated carbon (ZnO/AC) is discussed throughout this paper.

2. Methodology

2.1. Preparation of wood waste-derived activated carbon (AC)

AC was prepared according to our previous study [25]. In brief, the wood waste was collected from one of the wood-mill in Pahang and was washed with deionized water 4 to 5 times to remove dirt and dust particles to prevent contamination. The wood wastes were crushed into powder and dried (70 °C, 12 h). Then, the dried material was mixed with 36 wt% phosphoric acids, H_3PO_4, and kept at atmospheric temperature for one day by stirring occasionally. Next, the sample was calcined (500 °C, 2 h) in a furnace with nitrogen flow (150 mL/min). The sample was then rinsed multiple times with deionized water to remove surface-bound acid before being dried overnight at 110 °C. For practical usage, the dried sample was stored in an airtight container.

2.2. Preparation of ZnO/AC

ZnO/AC was prepared by an incipient wetness impregnation approach by adding the AC into a solution of 4 wt% $Zn(NO_3)_2{\cdot}6H_2O$ (Merck, 99%). The mixture was stirred at 80 °C until all water evaporated. The obtained slurry was oven-dried (110 °C, 12 h) and calcined (500 °C, 4 h).

2.3. Characterization of ZnO/AC

The X-ray diffraction (XRD) analysis was conducted in the range of $2\theta = 0.5° - 80°$ using RIGAKU XRD (Miniflex II, 15 mA, 30 kV). The functional groups of the sample were analyzed using PerkinElmer Spectrum GX Thermo Fisher Fourier Transform Infrared (FTIR) spectrometer in the range of 400–4000 cm^{-1}. Meanwhile, photoluminescence spectroscopy (PL) analysis was carried out using Edinburgh Instruments to observe material imperfections, impurities and to determine the electronic bandgap and absorbance spectrum of ZnO/AC. Additionally, ultraviolet–visible-near-IR spectroscopy (UV–Vis-NIR) analysis was carried out using Shimadzu UV-26900 UV–Vis-NIR Spectrophotometer to examine the absorption of light across the desired optical range of ZnO/AC.

2.4. Photocatalytic experiment

The degradation of MB solution in the presence of visible light was conducted to investigate the photocatalytic activity of ZnO supported on activated carbon. The experiment was carried out by adding a specific amount of ZnO/AC into 200 mL of MB solution in a batch reactor fixed with visible light (420 nm) and a cooling system. To reach adsorption–desorption equilibrium, the suspension was agitated at 700 rpm for 30 min in the dark, and then the suspension was irradiated for 4 h more for photocatalytic reaction. At a regular interval, 4 mL of the suspension was withdrawn and centrifuged (12,000 rpm, 10 min). The solution was monitored using a UV–VIS spectrometer to measure the absorbance at a wavelength of 664 nm. In this study, experiments were carried out with various parameters, including effects of pH (2 – 8), time (0 – 240 min), photocatalyst dosage (0.1 – 5 g/L), and initial MB concentration (10 – 100 mg/L). Equation (1) was used to compute the MB degradation efficiency.

$$MB\ Degradation\ (\%) = \frac{C_o - C_t}{C_o} \times 100 \quad (1)$$

where C_o is the initial MB concentration at $t = 0$ (mg/L) and C_t is the MB concentration at a given time (mg/L).

3. Result and discussion

3.1. Characterization of ZnO/AC

Fig. 1 shows the XRD pattern of ZnO/AC. Five prominent diffraction peaks were observed at $2\theta = 31.76°$, 34.41°, 36.24°, 47.53°, and 56.58°, respectively, which strongly matched with the diffraction planes (100), (002), (101), (102), and (110), correspondingly, as described in the standard spectrum of ZnO (JCPDS No. 01–089-0510). The peaks confirmed the formation of a crystalline hexagonal wurtzite structure of the ZnO [26]. The appearance of these sharp diffraction peaks signified the high crystallinity of the prepared ZnO/AC catalyst, which can increase the photocatalysis activity of ZnO/AC by limiting e^-/h^+ pair recombination and generating more reactive species for efficient reactions with MB molecules. Additionally, the XRD spectra of ZnO/AC revealed the successful impregnation of ZnO onto the AC. The high surface area

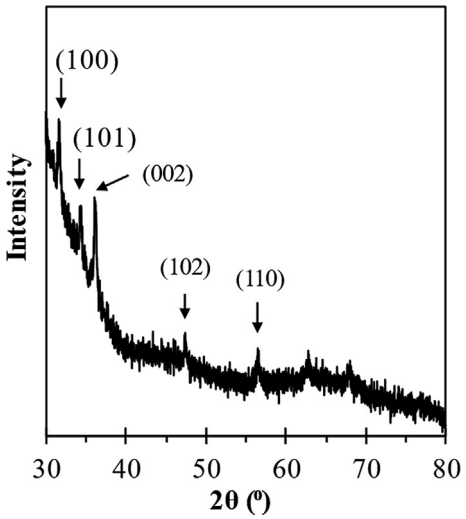

Fig. 1. XRD pattern of ZnO/AC.

of AC (1196 m^2/g) [25] results in good distribution of ZnO onto the AC.

Fig. 2 shows the FTIR spectra of AC and ZnO/AC. As previously reported [25], AC showed peaks at 2344 cm^{-1}, 2076 cm^{-1}, 1544 cm^{-1}, 950 cm^{-1}, and 447 cm^{-1}, corresponds to the broadening of the C-C double bond which originated from the COOH group, C-C triple bond stretching, C = H bending and C = C ring stretching mode of benzene derivatives, stretching vibrations of O-C associated with P-O-C linkage, H bonded of P = O and P = OOH, and C–H out-of-plane bending of benzene derivatives, respectively. The introduction of Zn develops a new peak at 1559 cm^{-1}, 1013 cm^{-1}, and 550 cm^{-1} corresponds to C = C stretching, O-H stretching of H_2O in C-O-Zn lattice, and stretching of ZnO in ZnO lattice [27]. This result indicates the successful incorporation of Zn onto AC.

To scrutinize the separation efficiency of photogenerated charge carriers, PL analysis of ZnO/AC was performed, and the spectra are shown in Fig. 3(a). In general, the peak observed is usually attributed to the band gap transition or exciton recombination of the catalyst, whereby the weak intensity of the peak indicates a high separation efficiency of photogenerated carriers [28]. As shown, the intensity of the peak increases with an increase in the excitation wavelength from 300 nm to 400 nm, indicating high separation efficiency by using a lower excitation wavelength. In contrast, Fig. 3(b) represents the optical band gap of ZnO/AC, which was evaluated using the Tauc plot. The value for ZnO/AC was found to be 2.5 eV, whereas 3.26 eV for ZnO was reported in the literature [29]. As shown, the band gap appears to be narrow, which is closely related to the oxygen vacancy. Gao et al. [30] reported that the band gap decreases as the carbon content increases, enhancing photocatalytic performance since carbon suppresses the recombination of electron-hole pairs upon absorption.

3.2. Photodegradation of MB

Fig. 4 shows the effect of time (0 – 240 min) on the degradation of MB using ZnO/AC. The degradation of MB was seen to increase with increasing contact time, reaching a maximum of around 180 min with MB degradation of 89.73%. Beyond 180 min, the MB degradation was observed to remain constant. High percentage degradation of MB revealed that ZnO/AC has considerable active sites that are able to carry out the degradation reaction in the presence of visible light.

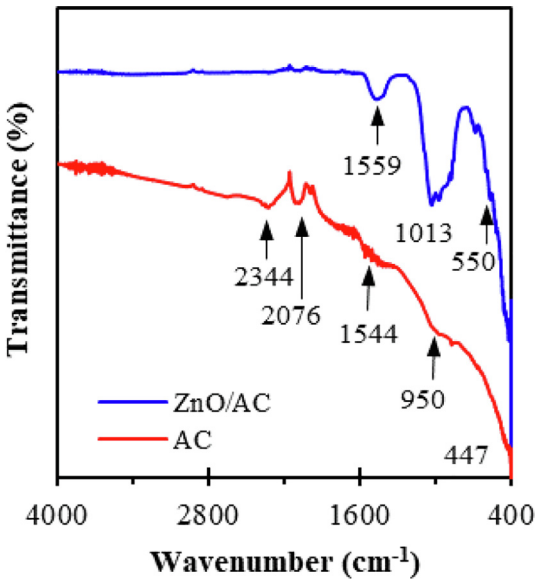

Fig. 2. FTIR spectra of AC and ZnO/AC.

Fig. 5 illustrates the effect of ZnO/AC dosage (0.1 – 5 g/L) on MB degradation. As observed, the MB degradation rate rose as the ZnO/AC dosage was increased, owing to an overabundance of photocatalytic sites. The higher number of active sites leads to an increase in the number of $^{\bullet}OH$ radicals, resulting in more significant interaction with the MB molecules [31]. At ZnO/AC dosage of 3 g/L, the degradation was 93.84%, and towards 5 g/L, no significant changes were observed. From this study, 3 g/L of ZnO/AC is sufficient to maximize overall MB degradation. Murugesan et al. [25] found a similar finding, in which MB degradation increased as the photocatalyst dose was raised, but no significant alterations were seen once the sufficient dosage was achieved.

Fig. 6 shows the effect of pH (2 – 8) on the degradation of MB using ZnO/AC. pH has a significant influence on the photocatalytic degradation process since it affects the charge of the catalyst surface and the dissociation of the dye molecules. At pH 2, the environment was saturated with the surplus of H^+ ions, thus hindering the adsorption and photodegradation of MB molecules. However, the number of positive charges on the catalyst surface reduced as the pH of the system increased from pH 2 to pH 6, enhancing the attraction of MB to the ZnO/AC surface. The number of negatively charged sites in the system increases as the pH rises, favoring the adsorption of MB cations onto the photocatalyst surface due to electrostatic attraction. This phenomenon results in higher MB degradation at pH 8. A similar phenomenon on the influence of pH toward the degradation percentage of MB was reported by Moalem et al. [32] for MB degradation over ZnO catalyst.

Fig. 7 illustrates the effect of the initial concentration of MB (10 – 100 mg/L) toward MB degradation using ZnO/AC. An increase in MB concentration from 10 mg/L to 100 mg/L slightly decreased the percentage of MB degradation from 100% to 97.94%. As the initial dye concentration increases, the photons entering solutions subsequently decrease due to the decrease of the path length, which results in lower adsorption for the photon on the catalyst particles, and consequently reduces the degradation efficiency [33]. A similar phenomenon on the influence of initial concentration toward degradation percentage of MB was reported by Calzada et al. [33] for MB degradation over ZnO/SBA-15 catalyst.

The kinetic study of photocatalytic degradation of MB using Zn/AC was modeled by Langmuir-Hinshelwood pseudo-first-order kinetic model [34]. The model assumes a direct proportion between the occupation rate of adsorption sites with the number of unoccupied sites. Generally, the Langmuir-Hinshelwood pseudo-first-order equation is expressed as follows (2):

$$\ln\left(\frac{C_o}{C_t}\right) = kt \tag{2}$$

where C_o (mg/L) is the initial MB concentration, C_t (mg/L) is the concentration of the MB at time t, k is the reaction rate constant (min^{-1}), and t is the irradiation time (min).

The kinetic constants, k, were calculated from the regression equation and are tabulated in Table 1. From the results obtained, the correlation coefficient (R^2) is 0.995 – 0.999. Therefore, the photocatalytic degradation of MB by ZnO/AC well fitted the Langmuir-Hinshelwood pseudo-first-order kinetic model. Djebri et al. [31], Shrestha et al. [16], Wu et al. [35] and Hung et al. [36] reported similar results, whereby the photocatalytic processes are well fitted with Langmuir-Hinshelwood pseudo-first-order kinetic model.

As reported in the literature [37], the degradation reaction mainly depends on the photon-generated electron-hole recombination concentration. In short, the presence of ZnO in the ZnO/AC hinders the electron-hole recombination and significantly

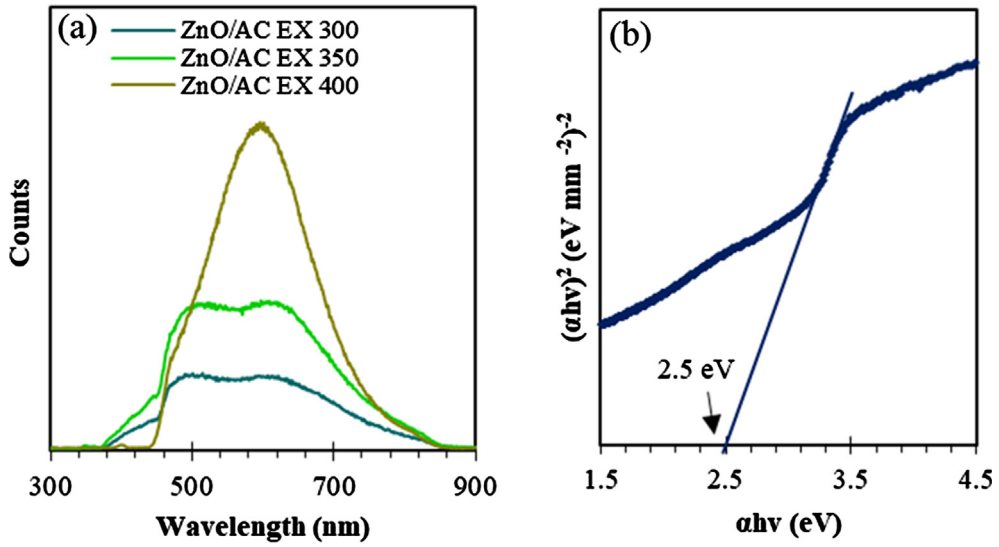

Fig. 3. (a) Photoluminescence spectra of ZnO/AC at different excitation wavelengths. (b) Band gap of ZnO/AC.

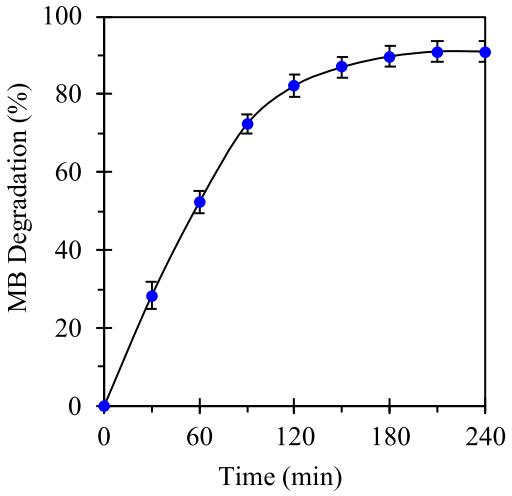

Fig. 4. Effect of time on methylene blue using ZnO/AC. Condition: C_o = 100 mg/L, pH = 6, and T = 30 °C. (For interpretation of the references to colour in this figure legend, the reader is referred to the web version of this article.)

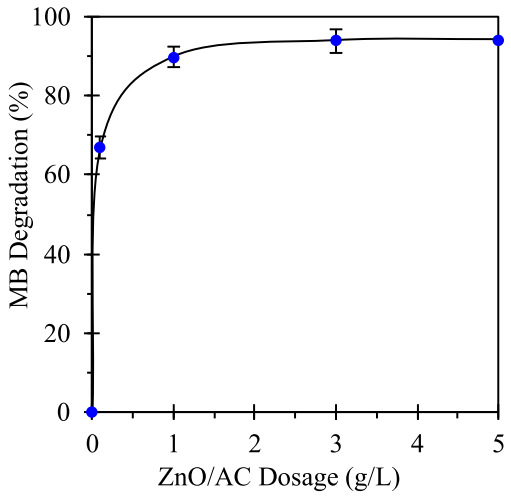

Fig. 5. Effect of catalyst dosage of ZnO/AC. Condition: C_o = 100 mg/L, pH = 6, t = 180 min, and T = 30 °C.

enhances the photocatalytic activity. Accordingly, that the excitation of ZnO/AC under visible light can be displayed in the following Equations (3)-(9). As the recombination of excited electrons reduced, the excited electron trap was completed by the activated carbon and oxygen sites of formation of superoxide ($O_2^{\bullet -}$), as shown in Equation (5)-(7). At last, $OH^\bullet$ and $O_2^{\bullet -}$ radicals are decomposed by the surface adsorbed MB dye as shown in Equations (8) and (9).

$$ZnO\ (VB) + hv \rightarrow ZnO\ (h^+\ VB) + ZnO\ (e^-\ CB) \quad (3)$$

$$ZnO\ (h^+\ VB) + H_2O \rightarrow OH^\bullet \quad (4)$$

$$ZnO\ (e^-\ CB) \rightarrow AC^\bullet \quad (5)$$

$$ZnO\ (e^-\ CB) + O_2 \rightarrow O_2^{\bullet -} \quad (6)$$

$$AC^\bullet + O_2 \rightarrow O_2^{\bullet -} \quad (7)$$

$$O_2^{\bullet -} + MB \rightarrow CO_2 + H_2O \quad (8)$$

$$OH^\bullet + MB \rightarrow CO_2 + H_2O \quad (9)$$

The catalyst's degradation performance was found to be impacted by the type of catalyst, pH, dye concentration, catalyst loading, and time. Table 2 shows the comparison of photocatalytic activity of ZnO/AC with recently reported ZnO-based catalysts for MB degradation. In short, the MB degradation is more than 76% with the presence of ZnO, proving the capability of Zn-based catalysts for the degradation of MB. The positive role of ZnO is due to its outstanding chemical stability, non-toxic nature, long-term-photostability, excellent charge transport properties, high UV absorbing properties [38], and large surface area [20]. The large surface area of ZnO enables more contaminants to be adsorbed onto its surface area and thus leads to more pollutants being attacked by hydroxyl radicals [20].

It was also observed that the MB degradation achieved more than 98% for the ZnO/$NiFe_2O_4$, ZnO/Eu_2O_3/NiO, and N/La-ZnO. However, these catalysts contain more than one type of metal that

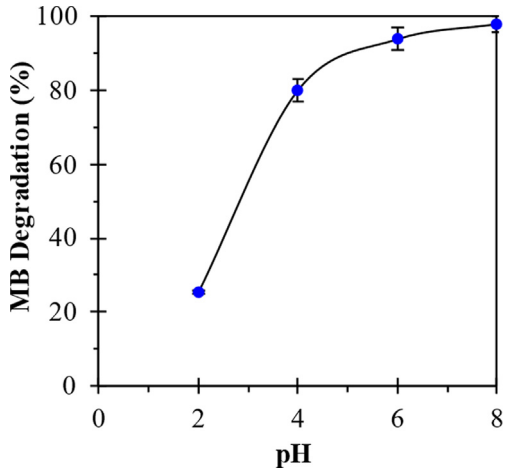

Fig. 6. Effect of pH on methylene blue using ZnO/AC. Condition: C_o = 100 mg/L, m = 3 g/L, t = 180 min, and T = 30 °C. (For interpretation of the references to colour in this figure legend, the reader is referred to the web version of this article.)

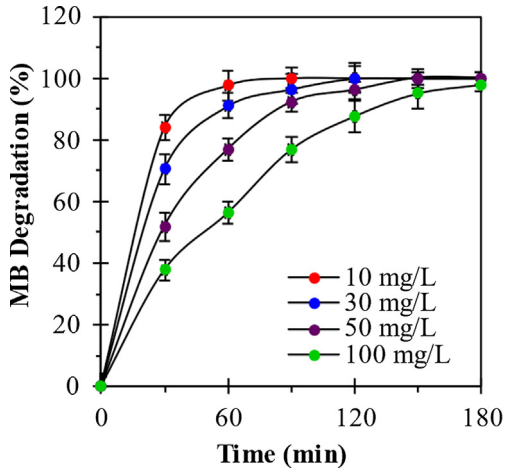

Fig. 7. Effect of initial concentration of methylene blue using ZnO/AC. Condition: m = 3 g/L, t = 180 min, pH = 8, and T = 30 °C. (For interpretation of the references to colour in this figure legend, the reader is referred to the web version of this article.)

Table 1
Kinetic Parameters for photocatalytic degradation of MB using ZnO/AC.

Concentration (g/L)	Langmuir-Hinshelwood model	
	k_1(min^{-1})	R^2
10	0.0621	0.999
30	0.0383	0.999
50	0.0269	0.998
100	0.0165	0.995

involves a high production cost compared to the ZnO/AC. Other than that, ZnO also tends to agglomerate during synthesization. Nevertheless, with the presence of activated carbon, the agglomeration is able to minimize. Hence, the formation of ZnO/AC can improve the uniformity of the spread of particles, leading to lower porosity and increasing the distribution of ZnO, resulting in a more homogenous layer. Consequently, the presence of AC overcomes the agglomeration of ZnO, leading to a more effective MB degradation [39]. In short, it can be suggested that ZnO/AC demonstrated excellent photocatalytic activity for the degradation of MB when compared to other catalysts while also being cost-effective.

Although the activated carbon has recently been shown to have photocatalytic activity alone when irradiated with visible light [40], the presence of activated carbon coupled with ZnO is able to enhance the splitting of the photogenerated exciton, resulting in high pollutant degradation [41]. In addition, the presence of activated carbon as support material in photocatalytic systems can improve the transfer rate of the interface charge and lower the recombination rate of holes and electrons [42]. With the above-mentioned advantages, AC has been considered promising support for the design and synthesis of ZnO/AC in removing MB from wastewater.

4. Conclusion

The incipient wetness impregnation method was utilized to successfully prepare ZnO/AC catalyst from wood waste, which was then used for MB degradation using visible light. The characterization results of FTIR and PL revealed that ZnO/AC formed wells, and XRD data proved the presence of hexagonal wurtzite crystal structure in ZnO. The optimal ZnO/AC conditions were attained after 180 min, photocatalyst dosage of 3 g/L, and pH 8. Complete MB degradation was observed at lower dye concentrations (10 – 50 mg/L), and the performance was slightly decreased at higher MB concentration (100 mg/L). The photocatalytic kinetics well fitted with the Langmuir-Hinshelwood pseudo-first-order model with an R^2 value of 0.995 – 0.999, indicating a bimolecular reaction between two species available on the catalyst's surface. The results showed that the prepared ZnO/AC had outstanding catalytic activity in the degradation of MB when exposed to visible light. In the continuity of this study, the reusability and regeneration of ZnO/SBA-15 toward MB degradation can be further studied. In addition, photocatalytic activities can be further investigated using industrial wastewater containing MB.

CRediT authorship contribution statement

J.Y. Loke: Investigation, Writing – original draft. **R.S. Mohd Zaki:** Investigation, Writing – original draft. **H.D. Setiabudi:** Conceptualization, Supervision, Project administration, Writing – review & editing.

Table 2
Comparison of photocatalytic activity of ZnO/AC with recently reported ZnO-based catalysts for MB degradation.

Catalyst	Dye	Dye concentration (mg/L)	Catalyst dosage (g/L)	Light source	pH	Time (min)	Dye degradation (%)	Ref
ZnO/AC	MB	50	3.00	Visible light (420 nm)	8	180	100	This study
ZnO/NWs	MB	100	0.10	Sunlight irradiation	–	4320	100	[43]
ZnO/$NiFe_2O_4$	MB	50	0.08	UV light (360 nm)	–	70	98	[26]
ZnO/Eu_2O_3/NiO	MB	50	0.03	UV light (370 nm)	10	150	98	[44]
ZnO-SiO_2	MB	100	0.10	Sunlight irradiation	–	180	97.8	[3]
N/La-ZnO	MB	200	0.50	Sunlight irradiation	–	60	97	[45]
Fe-ZnO	MB	100	1.00	Visible light (550 nm)	2	140	92	[46]
ZnO/$ZnFe_2O_4$	MB	100	0.10	Visible light (420 nm)	–	140	91.2	[47]
ZnO/CeO_2	MB	100	3.00	Visible light (420 nm)	8	180	84	[48]
Ag/ZnO	MB	100	0.10	Visible light (420 nm)	–	240	76	[49]

Declaration of Competing Interest

The authors declare that they have no known competing financial interests or personal relationships that could have appeared to influence the work reported in this paper.

Acknowledgment

This study was supported by Universiti Malaysia Pahang through the UMP International Publication Grant (RDU203303).

References

[1] S. Varjani, P. Rakholiya, H.Y. Ng, S. You, J.A. Teixeira, Microbial degradation of dyes: An overview, Bioresour. Technol. 314 (2020) 123728, https://doi.org/10.1016/j.biortech.2020.123728.
[2] R. Foroutan, R. Mohammadi, J. Razeghi, B. Ramavandi, Performance of algal activated carbon/Fe 3 O 4 magnetic composite for cationic dyes removal from aqueous solutions, Algal Res. 40 (2019) 101509, https://doi.org/10.1016/j.algal.2019.101509.
[3] S. R, A.J. J, M.V. S, Enhanced sunlight photocatalytic degradation of methylene blue by rod-like ZnO-SiO2 nanocomposite, Optik 180 (2019) 134–143, https://doi.org/10.1016/j.ijleo.2018.11.084.
[4] A. Othmani, A. Kesraoui, M. Seffen, The alternating and direct current effect on the elimination of cationic and anionic dye from aqueous solutions by electrocoagulation and coagulation flocculation, Euro-Mediterranean J. Environ. Integration 2 (1) (2017) 1–12, https://doi.org/10.1007/s41207-017-0016-y.
[5] L. Mouni, L. Belkhiri, J.-C. Bollinger, A. Bouzaza, A. Assadi, A. Tirri, F. Dahmoune, K. Madani, H. Remini, Removal of Methylene Blue from aqueous solutions by adsorption on Kaolin: Kinetic and equilibrium studies, Appl. Clay Sci. 153 (2018) 38–45, https://doi.org/10.1016/j.clay.2017.11.034.
[6] S. Liu, G. Pan, H. Yang, Z. Cai, F. Zhu, G. Ouyang, Determination and elimination of hazardous pollutants by exploitation of a Prussian blue nanoparticles-graphene oxide composite, Anal. Chim. Acta 1054 (2019) 17–25, https://doi.org/10.1016/j.aca.2018.12.011.
[7] H. Ahmari, S.Z. Heris, M.H. Khayyat, The effect of titanium dioxide nanoparticles and UV irradiation on photocatalytic degradation of Imidaclopride, Environm. Technol. (United Kingdom) 39 (4) (2018) 536–547, https://doi.org/10.1080/09593330.2017.1306115.
[8] O. Fawzi, S. Khasawneh, P. Palaniandy, Environmental Technology & Innovation Removal of organic pollutants from water by Fe 2 O 3 / TiO 2 based photocatalytic degradation : A review, Environ. Technol. Innovation (2020), https://doi.org/10.1016/j.eti.2020.101230 101230.
[9] A. Modwi, B. Mustafa, M. Ismail, S.Z.A. Makawi, T.I. Hussein, Z.M. Abaker, A. Mujawah, A.S. Al-Ayed, Physicochemical and photocatalytic performance of the synthesized RuO2-ZnO photo-composite in the presence of pectinose solution, Environ. Nanotechnol. Monit. Manage. 15 (2021) 100403, https://doi.org/10.1016/j.enmm.2020.100403.
[10] L. Cheng, S. Liu, G. He, Y. Hu, The simultaneous removal of heavy metals and organic contaminants over a Bi2WO6/mesoporous TiO2 nanotube composite photocatalyst, RSC Adv. 10 (36) (2020) 21228–21237.
[11] C. Hao, Y. Liao, Y. Wu, Y. An, J. Lin, Z. Gu, M. Jiang, S. Hu, X. Wang, RuO2-loaded TiO2–MXene as a high performance photocatalyst for nitrogen fixation, J. Phys. Chem. Solids 136 (2020) 109141, https://doi.org/10.1016/j.jpcs.2019.109141.
[12] X. Hu, G. Wang, J. Wang, Z. Hu, and Y. Su, "Step-scheme NiO/BiOI heterojunction photocatalyst for rhodamine photodegradation," *Applied Surface Science*, vol. 511, no. October 2019, p. 145499, 2020, doi: 10.1016/j.apsusc.2020.145499.
[13] A. Raja, P. Rajasekaran, K. Selvakumar, M. Arunpandian, K. Kaviyarasu, S. Asath Bahadur, M. Swaminathan, Visible active reduced graphene oxide-BiVO4-ZnO ternary photocatalyst for efficient removal of ciprofloxacin, Sep. Purif. Technol. 233 (2020) 115996, https://doi.org/10.1016/j.seppur.2019.115996.
[14] E. Kusmierek, A CeO2 semiconductor as a photocatalytic and photoelectrocatalytic material for the remediation of pollutants in industrial wastewater: A review, Catalysts 10 (12) (2020) 1–54, https://doi.org/10.3390/catal10121435.
[15] M.A. Ahmed, Z.M. Abou-Gamra, A.M. Salem, Photocatalytic degradation of methylene blue dye over novel spherical mesoporous Cr2O3/TiO2 nanoparticles prepared by sol-gel using octadecylamine template, J. Environ. Chem. Eng. 5 (5) (2017) 4251–4261, https://doi.org/10.1016/j.jece.2017.08.014.
[16] P. Shrestha, M.K. Jha, J. Ghimire, A.R. Koirala, R.M. Shrestha, R.K. Sharma, B. Pant, M. Park, H.R. Pant, Decoration of zinc oxide nanorods into the surface of activated carbon obtained from agricultural waste for effective removal of methylene blue dye, Materials 13 (24) (2020) 5667, https://doi.org/10.3390/ma13245667.
[17] F. Azeez, E. Al-Hetlani, M. Arafa, Y. Abdelmonem, A.A. Nazeer, M.O. Amin, M. Madkour, The effect of surface charge on photocatalytic degradation of methylene blue dye using chargeable titania nanoparticles, Sci. Rep. 8 (1) (2018), https://doi.org/10.1038/s41598-018-25673-5.
[18] C. Karthikeyan, P. Arunachalam, K. Ramachandran, A.M. Al-Mayouf, S. Karuppuchamy, Recent advances in semiconductor metal oxides with enhanced methods for solar photocatalytic applications, J. Alloy. Compd. 828 (2020) 154281, https://doi.org/10.1016/j.jallcom.2020.154281.
[19] C.B. Ong, L.Y. Ng, A.W. Mohammad, A review of ZnO nanoparticles as solar photocatalysts: Synthesis, mechanisms and applications, Renew. Sustain. Energy Rev. 81 (2018) 536–551.
[20] C. B. Ong, L. Y. Ng, and A. W. Mohammad, "A review of ZnO nanoparticles as solar photocatalysts: Synthesis, mechanisms and applications," *Renewable and Sustainable Energy Reviews*, vol. 81, no. July 2016, pp. 536–551, 2018, doi: 10.1016/j.rser.2017.08.020.
[21] R.I. Kosheleva, A.C. Mitropoulos, G.Z. Kyzas, Synthesis of activated carbon from food waste, Environ. Chem. Lett. 17 (1) (2019) 429–438, https://doi.org/10.1007/s10311-018-0817-5.
[22] M. Lewoyehu, Comprehensive review on synthesis and application of activated carbon from agricultural residues for the remediation of venomous pollutants in wastewater, J. Anal. Appl. Pyrol. 159 (2021) 105279, https://doi.org/10.1016/j.jaap.2021.105279.
[23] K. Yu, H. Zhu, H. Qi, C. Liang, High surface area carbon materials derived from corn stalk core as electrode for supercapacitor, Diam. Relat. Mater. 88 (Sep. 2018) 18–22, https://doi.org/10.1016/j.diamond.2018.06.018.
[24] J. Elisadiki, Y.A.C. Jande, R.L. Machunda, T.E. Kibona, Porous carbon derived from Artocarpus heterophyllus peels for capacitive deionization electrodes, Carbon 147 (Jun. 2019) 582–593, https://doi.org/10.1016/j.carbon.2019.03.036.
[25] C.Q. Teong, H.D. Setiabudi, N.A.S. El-Arish, M.B. Bahari, L.P. Teh, Vatica rassak wood waste-derived activated carbon for effective Pb(II) adsorption: Kinetic, isotherm and reusability studies, Mater. Today:. Proc. 42 (2019) 165–171, https://doi.org/10.1016/j.matpr.2020.11.270.
[26] J. T. Adeleke, T. Theivasanthi, M. Thiruppathi, M. Swaminathan, T. Akomolafe, and A. B. Alabi, "Photocatalytic degradation of methylene blue by ZnO/NiFe 2 O 4 nanoparticles," *Applied Surface Science*, vol. 455, no. September 2017, pp. 195–200, 2018, doi: 10.1016/j.apsusc.2018.05.184.
[27] Y. Kumar, A. Sahai, S.F. Olive-Méndez, N. Goswami, V. Agarwal, Morphological transformations in cobalt doped zinc oxide nanostructures: Effect of doping concentration, Ceram. Int. 42 (4) (Mar. 2016) 5184–5194, https://doi.org/10.1016/j.ceramint.2015.12.041.
[28] C.N.C. Hitam, A.A. Jalil, Y.O. Raji, Fabrication of Fibrous Silica Zinc (FSZn) Composite for Enhanced Photocatalytic Desulphurization, Top. Catal. 63 (11–14) (2020) 1169–1181, https://doi.org/10.1007/s11244-020-01275-2.
[29] S.S. Mydeen, R.R. Kumar, S. Sambathkumar, M. Kottaisamy, V.S. Vasantha, Facile Synthesis of ZnO/AC Nanocomposites using Prosopis Juliflora for Enhanced Photocatalytic Degradation of Methylene Blue and Antibacterial Activity, Optik 224 (2020) 165426, https://doi.org/10.1016/j.ijleo.2020.165426.
[30] X. Gao, P.-G. Ren, J. Wang, F. Ren, Z. Dai, Y.-L. Jin, Fabrication of visible-light responsive TiO2@C photocatalyst with an ultra-thin carbon layer to efficiently degrade organic pollutants, Appl. Surf. Sci. 532 (2020) 147482, https://doi.org/10.1016/j.apsusc.2020.147482.
[31] A. Djebri, M. Belmedani, B. Belhamdi, M. Trari, Z. Sadaoui, The combined effectiveness of activated carbon (AC) / ZnO for the adsorption of mebeverine hydrochloride / photocatalytic degradation under sunlight, Reaction Kinetics, Mechanisms and Catalysis 132 (1) (2021) 529–546, https://doi.org/10.1007/s11144-021-01932-x.
[32] M. Moalem-Banhangi, N. Ghaeni, S. Ghasemi, Saffron derived carbon quantum dot/N-doped ZnO/fulvic acid nanocomposite for sonocatalytic degradation of methylene blue, Synth. Met. 271 (2021) 116626, https://doi.org/10.1016/j.synthmet.2020.116626.
[33] L.A. Calzada, R. Castellanos, L.A. García, T.E. Klimova, TiO2, SnO2 and ZnO catalysts supported on mesoporous SBA-15 versus unsupported nanopowders in photocatalytic degradation of methylene blue, Micropor. Mesopor. Mater. 285 (Sep. 2019) 247–258, https://doi.org/10.1016/j.micromeso.2019.05.015.
[34] R. Subagyo, Y. Kusumawati, and W. B. Widayatno, "Kinetic study of methylene blue photocatalytic decolorization using zinc oxide under UV-LED irradiation," *AIP Conference Proceedings*, vol. 2237, no. June, 2020, doi: 10.1063/5.0005263.
[35] F. Wu, X. Li, W. Liu, S. Zhang, Highly enhanced photocatalytic degradation of methylene blue over the indirect all-solid-state Z-scheme g-C 3 N 4 -RGO-TiO 2 nanoheterojunctions, Appl. Surf. Sci. 405 (2017) 60–70, https://doi.org/10.1016/j.apsusc.2017.01.285.
[36] N. Van Hung, B.T.M. Nguyet, N.H. Nghi, D.Q. Khieu, Photocatalytic Degradation of Methylene Blue by Using ZnO/Longan Seed Activated Carbon Under Visible-Light Region, J. Inorg. Organomet. Polym Mater. 31 (1) (2021) 446–459, https://doi.org/10.1007/s10904-020-01734-z.
[37] R. Ranjith, V. Renganathan, S.M. Chen, N.S. Selvan, P.S. Rajam, Green synthesis of reduced graphene oxide supported TiO 2 /Co 3 O 4 nanocomposite for photocatalytic degradation of methylene blue and crystal violet, Ceram. Int. 45 (10) (Jul. 2019) 12926–12933, https://doi.org/10.1016/j.ceramint.2019.03.219.
[38] N. Justh, L.P. Bakos, K. Hernádi, G. Kiss, B. Réti, Z. Erdélyi, B. Parditka, I.M. Szilágyi, Photocatalytic hollow TiO2 and ZnO nanospheres prepared by atomic layer deposition, Sci. Rep. 7 (1) (2017), https://doi.org/10.1038/s41598-017-04090-0.
[39] D.R. Eddy, A.R. Noviyanti, S. Solihudin, S. Ishmayana, R.-A. Tjokronegoro, Rice Husk for Photocatalytic Composite Material Fabrication, in: Y. Yao (Ed.), Visible-Light Photocatalysis of Carbon-Based Materials, InTech, 2018, https://doi.org/10.5772/intechopen.72704.

[40] V. Sydorchuk, O.I. Poddubnaya, M.M. Tsyba, O. Zakutevskyy, O. Khyzhun, S. Khalameida, A.M. Puziy, Photocatalytic degradation of dyes using phosphorus-containing activated carbons, Appl. Surf. Sci. 535 (2021) 147667, https://doi.org/10.1016/j.apsusc.2020.147667.
[41] A. Gomis-Berenguer, L.F. Velasco, I. Velo-Gala, C.O. Ania, Photochemistry of nanoporous carbons: Perspectives in energy conversion and environmental remediation, J. Colloid Interface Sci. 490 (2017) 879–901, https://doi.org/10.1016/j.jcis.2016.11.046.
[42] G.Z. Kyzas, G. Bomis, R.I. Kosheleva, E.K. Efthimiadou, E.P. Favvas, M. Kostoglou, A.C. Mitropoulos, Nanobubbles effect on heavy metal ions adsorption by activated carbon, Chem. Eng. J. 356 (2019) 91–97, https://doi.org/10.1016/j.cej.2018.09.019.
[43] A. Mahana, O.I. Guliy, S.C. Momin, R. Lalmuanzeli, S.K. Mehta, Sunlight-driven photocatalytic degradation of methylene blue using ZnO nanowires prepared through ultrasonication-assisted biological process using aqueous extract of Anabaena doliolum, Opt. Mater. 108 (2020) 110205, https://doi.org/10.1016/j.optmat.2020.110205.
[44] J.P. Shubha, S.F. Adil, M. Khan, M.R. Hatshan, A. Khan, Facile Fabrication of a ZnO/Eu2O3/NiO-Based Ternary Heterostructure Nanophotocatalyst and Its Application for the Degradation of Methylene Blue, ACS Omega 6 (5) (2021) 3866–3874, https://doi.org/10.1021/acsomega.0c05670.
[45] A.M. Youssef, S.M. Yakout, Superior sunlight photocatalytic of N/La codoped ZnO nanostructures synthesized using different chelating agents, Opt. Mater. 107 (2020) 110072, https://doi.org/10.1016/j.optmat.2020.110072.
[46] K.A. Isai, V.S. Shrivastava, Photocatalytic degradation of methylene blue using ZnO and 2%Fe–ZnO semiconductor nanomaterials synthesized by sol–gel method: a comparative study, SN Applied Sciences 1 (10) (2019) 1–11, https://doi.org/10.1007/s42452-019-1279-5.
[47] M. Kuang, J. Zhang, W. Wang, J. Chen, R. Liu, S. Xie, J. Wang, Z. Ji, Synthesis of octahedral-like ZnO/ZnFe2O4 heterojunction photocatalysts with superior photocatalytic activity, Solid State Sci. 96 (2019) 105901, https://doi.org/10.1016/j.solidstatesciences.2019.05.012.
[48] H. Tju, H. Shabrany, A. Taufik, R. Saleh, Degradation of methylene blue (MB) using ZnO/CeO2/nanographene platelets (NGP) photocatalyst: Effect of various concentration of NGP, AIP Conf. Proc. 2017 (1862) 2017, https://doi.org/10.1063/1.4991141.
[49] M.F. Abdel Messih, M.A. Ahmed, A. Soltan, S.S. Anis, Synthesis and characterization of novel Ag/ZnO nanoparticles for photocatalytic degradation of methylene blue under UV and solar irradiation, J. Phys. Chem. Solids 135 (2019) 109086, https://doi.org/10.1016/j.jpcs.2019.109086.